Archaeal and bacterial glycerol dialkyl glycerol tetraether (GDGT) lipids in environmental samples by high temperature-gas chromatography with flame ionisation and time-of-flight mass spectrometry detection

Sabine K. Lengger [a,b,*], Paul A. Sutton [b], Steven J. Rowland [b], Sarah J. Hurley [c], Ann Pearson [c], B. David A. Naafs [a], Xinyue Dang [d], Gordon N. Inglis [a], Richard D. Pancost [a]

[a] Organic Geochemistry Unit and The Cabot Institute, School of Chemistry, University of Bristol, Bristol, UK
[b] Petroleum and Environmental Geochemistry Group, Biogeochemistry Research Centre, School of Geography, Earth and Environmental Sciences, University of Plymouth, Plymouth, UK
[c] Department of Earth and Planetary Sciences, Harvard University, Cambridge, MA, USA
[d] State Key Laboratory of Biogeology and Environmental Geology, School of Earth Science, China University of Geosciences, Wuhan 430074, China

ARTICLE INFO

ABSTRACT

Archaeal isoprenoidal glycerol dibiphytanyl glycerol tetraether lipids (iGDGTs) and their non-isoprenoidal branched bacterial analogues (brGDGTs) have widespread applications in biogeochemistry and paleothermometry. Analysis of GDGTs usually involves separation using high performance liquid chromatography, typically coupled via atmospheric pressure chemical ionisation to mass spectrometric detection in selected ion-monitoring mode (HPLC–APCI-MS). However, reliable determination of ratios and, in particular, quantification by this technique, can be challenging due to differences in ionisation efficiencies of the various compounds. Quantification of GDGTs also relies on external calibration of the relative response to an internal standard with authenticated GDGTs, which are often not readily accessible. Here, we tested the suitability of high temperature gas chromatography with flame ionisation detection (HTGC-FID) for the determination of concentrations and tetraether lipid-based ratios in marine and terrestrial samples. For this, we identified GDGTs in environmental samples using HTGC coupled to time-of-flight mass spectrometry (HTGC–MS). Using a purified GDGT standard, we show we can quantify GDGT-0 in environmental samples by GC-FID. Some GDGT-based ratios measured by HTGC-FID exhibited a linear correlation (1:1) with ratios derived from HPLC–MS and weight-based ratios of mixtures of purified standards. However, ratios relying on minor isomers, such as TEX_{86} and MBT/CBT have many unresolved challenges for determination by HTGC. Detection limits were higher than for HPLC–MS. However, the advantages of employing HTGC-based methods include: (1) the independence from MS tuning-related differences in ionisation energies; (2) the potential for direct comparison with other, non-GDGT based biomarkers; and (3) a more complete insight into biomarker distributions in environmental samples by the extension of the temperature range. Quantitative elution of GDGTs from a HTGC column as demonstrated herein, will also enable their analysis by compound-specific isotope ratio mass spectrometry.

© 2018 Elsevier Ltd. All rights reserved.

1. Introduction

Archaeal isoprenoidal glycerol dibiphytanyl tetraether lipids and the non-isoprenoidal, branched bacterial analogues (Fig. 1), are important classes of microbial biomarkers. Variations in their distributions serve as proxies for palaeotemperature (Schouten et al., 2002; Weijers et al., 2007), organic matter sources (Hopmans et al., 2004), and soil pH (Weijers et al., 2007; reviewed by Pearson and Ingalls, 2013; Schouten et al., 2013b).

Due to the relatively high molecular masses of GDGTs (Fig. 1; 1000 to >1300 Da), analysis is usually carried out using high performance liquid chromatography coupled with mass spectrometry via atmospheric pressure chemical ionisation (i.e., HPLC–APCI-MS; Hopmans et al., 2000; Schouten et al., 2007; Knappy et al., 2009) or electrospray ionisation interfaces (Zhu et al., 2013). Alternatively, chemical degradation of the ether bonds (Fig. 1) is applied to obtain hydrocarbons (biphytanes or branched alkanes), which are then analysed using gas chromatography coupled with MS (GC–MS; Sehgal et al., 1962; De Rosa and Gambacorta, 1988;
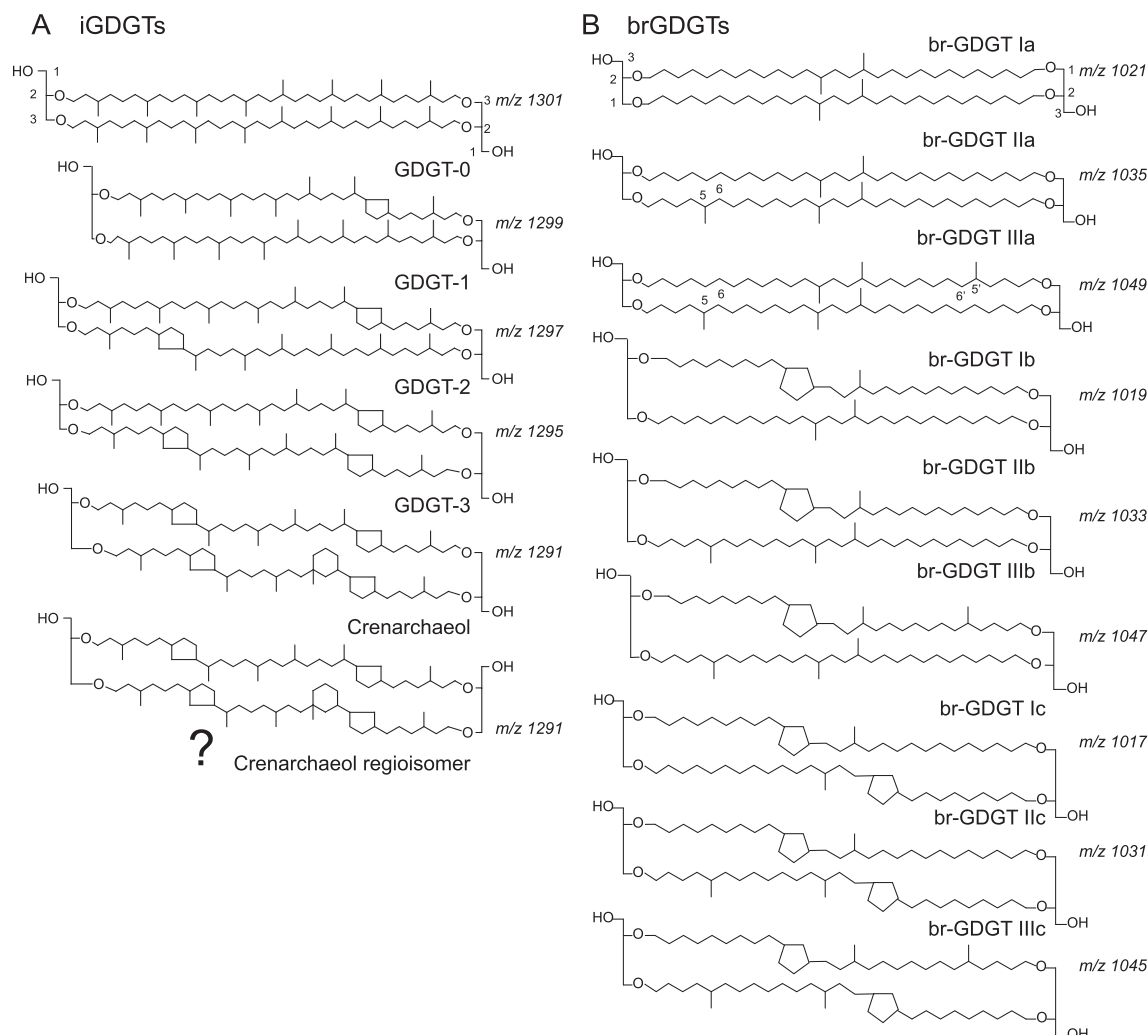
Fig. 1. Structures of GDGT molecules analysed in this study. A: iGDGTs, B: brGDGTs.

Schouten et al., 1998). However, due to the loss of structural information about the collocation of the biphytanes, it is not possible to use these moieties in proxy applications to reconstruct temperature or pH, and inconsistent reaction yields preclude their application as a quantitative proxy for organic matter (OM) sources.

Biogeochemical applications to date therefore are generally limited to HPLC–APCI-MS, which is often carried out in selected ion monitoring (SIM) mode (Schouten et al., 2007). This approach relies on measurement of the signal intensities of protonated molecules $[M+H]^+$ relative to an internal standard (Huguet et al., 2006), often producing semi-quantitative results due to the scarcity of authentic standards for external calibrations. Relative ionisation efficiencies for brGDGTs vs iGDGTs, in particular, can deviate and are largely dependent on tuning or instrument sensitivity, resulting in discrepancies in relative abundances (Schouten et al., 2009, 2013a). This is problematic, given the use of ratios between br-GDGTs and iGDGTs in order to distinguish OM sources (Branched over Isoprenoid Tetraether index, BIT; Hopmans et al., 2004). Recent efforts have been made towards improved chromatography (Hopmans et al., 2016), but also MS methods with higher mass resolution such as time-of-flight secondary ion MS (Sjövall et al., 2008), laser desorption coupled to Fourier-transform ion cyclotron resonance MS (Wörmer et al., 2014), and hybrid ion trap-orbitrap MS (Jensen et al., 2015). These methods allow the assignment of molecular formulae with high confidence;

yet they are not quantitative and are unable (without using chromatographic separation) to distinguish between isobaric structural isomers (e.g., of crenarchaeol; Fig. 1) and therefore cannot be used to measure established GDGT-based proxies.

We hypothesise that HTGC-FID, which has only been reported in limited cases to date, could provide a useful alternative for quantification of GDGTs. HTGC-FID was used by Nichols et al. (1993) for analysing GDGTs of a culture of *Thermoplasma acidophilum*. Weijers et al. (2006) and Pancost et al. (2001, 2008) used HTGC-FID for analysis of archaeal lipids in a microbial mat from a methane seep. However, in these cases, identification of the peaks was only inferred from retention times, based on the reasoning that increasing cyclisation would increase retention times, as observed with analogous biphytanes and by comparison to distributions determined by HPLC–APCI-MS. Sutton and Rowland (2012) were the first to analyse trimethylsilyl ethers of iGDGTs in lipid extracts of an archaeal culture (*Thermococcus waiotapuensis*) using HTGC coupled with time-of-flight-MS (HTGC–ToF-MS), and obtained electron ionisation (EI) mass spectra of such compounds for the first time, also including a spectrum of an unidentified, but potentially GDGT-like compound in a marine sediment.

Here, we apply the HTGC–MS method of Sutton and Rowland (2012) for analysis of environmental samples. We report, for the first time, the mass spectra and retention orders of the most abundant br- and iGDGTs in a marine sediment, a peat, and a cold seep

microbial mat. We use HTGC-FID for quantification of GDGTs, as well as to determine ratios used as environmental proxies which we compare to values determined via HPLC–APCI-MS. Our demonstration of a reliable HTGC-FID method for quantification of GDGTs has extensive applications. It will enable quantitative comparisons with other biomarkers and allow an evaluation of relative concentrations independent from mass spectrometric tuning settings. Further, the achievement of quantitative elution of GDGTs from a HTGC column should enable their analysis by compound-specific isotope ratio mass spectrometry.

2. Methodology

2.1. Samples used for GDGT identification

GDGT-0 and crenarchaeol standards (Fig. 1A) were purified previously from marine sediments, with concentrations confirmed both gravimetrically and by quantitative combustion to CO_2 (Pearson et al., 2016). Environmental samples consisted of: (1) an extract of an in-house prepared mixture of Paleogene marine sediments from Deep Sea Drilling Project (DSDP) sites 179 and 341, and from a section across the Cretaceous/Paleogene boundary at mid-Waipara, New Zealand (Taylor et al., 2013, 2018); (2) an extract of a peat from a Welsh ombrotrophic bog, Cors Caron (Hornibrook and Bowes, 2007); and (3) a carbonate sample derived

from methane seep in the Dnieper mouth of the Black Sea (Roberts et al., 2008).

2.2. Samples used for comparison of GDGT-derived ratios

All samples and relevant references for the determination of GDGT-derived ratios are summarised in Table 1. Marine surface sediments used for BIT index comparison (Hopmans et al., 2004) were collected from the Baltic Sea during the Metrol project (Aquilina et al., 2010; Table 1) and showed a large range of values (BIT: 0.07–0.82). Samples used for the determination of the methylation index of branched tetraethers and the cyclisation ratio of branched tetraethers (MBT-CBT, Weijers et al., 2007) were from soils (Dang et al., 2016), peat (Naafs et al., 2017) and lignites (Inglis et al., 2017) as outlined in Table 1, and again represent a large range. A sample from a Cretaceous sediment (Naafs et al., 2016) and the marine sediment mixture was used to determine the TetraEther indeX of tetraethers consisting of 86 carbon atoms, TEX_{86} (Schouten et al., 2002).

2.3. Extraction, purification and derivatisation

Samples were freeze-dried and extracted by Soxhlet extraction in dichloromethane/methanol (DCM/MeOH, 2:1, v:v) or a modified Bligh Dyer extraction (Bligh and Dyer, 1959; Lengger et al., 2012) to obtain a total lipid extract (TLE). All samples, except for the

Table 1

Provenance of samples used and results for the relative abundances of GDGTs as determined by GC as well as the ratios calculated by GC and LC. In brackets, mol-based values for BIT are given acc. under the assumption of a unit-carbon response of the FID. [1]Aquilina et al., 2010, [2]Taylor et al., 2013, 2018 [3]Inglis et al., 2017, [4]Naafs et al., 2017, [5]Dang et al., 2016, [6]Naafs et al., 2016.

Reference/Provenance	Relative abundance/%										
BIT			brGDGTs	GDGT-0	Cren						BIT GC (LC)
Sk 808-5	Skagerrak[1]	GC	12.3	40.7	47						0.25 (0.21)
351 GC4 14	Western Baltic[1]	GC	16.2	35.6	48.3						0.29 (0.28)
GTVC59 #31	Kattegat[1]	GC	44.6	35.3	20.2						0.73 (0.65)
H820-3	Skagerrak	GC	10	48.1	41.9						0.23 (0.15)
GTVC59 # 59	Kattegat[1]	GC	100	0	0						1 (0.82)
GTGC28 #3	Skagerrak[1]	GC	30.2	38.8	31						0.55 (0.53)
GTGC28 #1	Skagerrak[1]	GC	28.8	43.7	27.5						0.57 (0.55)
GTGC28 #7	Skagerrak[1]	GC	30.5	38.6	30.8						0.55 (0.68)
H786-4	Skagerrak[1]	GC	7.3	48.2	44.5						0.17 (0.1)
H836-2	Skagerrak[1]	GC	9	51.2	39.8						0.22 (0.19)
Marine sediment	DSDP 179, 341, mid-Waipara K/Pg[2]	GC	6.8	39.5	53.7						0.14 (0.07)
MBT/CBT			br Ia	br Ib	br Ic	br IIa	br IIb	br IIc	br IIIa	br IIIb	br IIIc	MBT - CBT
Schoeningen	Eocene lignite[3]	GC	77.5	10.3	6.1	5.8	0.3	n.d.	n.d.	n.d.	n.d.	0.94–0.90
		LC	79.5	8.6	5.9	4.0	0.4	0.1	1.5	0.0	0.0	0.94–0.97
Iberia_221 Z20	Peat sample[4]	GC	50.8	3.1	n.d.	38.3	3.0	n.d.	4.8	n.d.	n.d.	0.54–1.17
		LC	52.5	1.4	0.7	40.8	0.7	0.3	3.6	0.0	0.0	0.55–1.7
Iberia_221 Z40	Peat sample[4]	GC	49.4	4.4	n.d.	31.8	6.3	1.2	2.3	3.6	1.0	0.54–0.89
		LC	49.0	6.8	2.1	34.6	3.6	0.8	3.1	0.0	0.0	0.58–0.91
EH-8	Chinese soil[5]	GC	10.0	15.0	n.d.	26.1	29.2	n.d.	19.0	0.8	n.d.	0.25 - –0.09
		LC	20.9	15.3	2.3	34.7	22.0	1.5	10.4	1.1	0.0	0.36–0.17
EH-26	Chinese soil[5]	GC	3.8	13.0	n.d.	26.4	28.2	n.d.	23.9	4.8	n.d.	0.17 - –0.01
		LC	15.0	14.1	2.5	25.9	24.6	1.8	13.7	2.2	0.1	0.32–0.03
Peat standard	Cors Caron	GC	34.9	6.2	0.0	43.0	4.5	0.0	11.5	0.0	0.0	0.41–0.14
		LC	40.3	3.7	0.8	43.7	1.5	0.7	9.0	0.2	0.0	0.44–0.06
FSEB	Indonesian peat[4]	GC	71.8	8.3	13.9	5.9	n.d.	n.d.	n.d.	n.d.	n.d.	0.94–0.97
		LC	94.2	1.8	2.0	1.2	n.d.	n.d.	0.7	0.1	n.d.	0.98–1.73
TEX₈₆			GDGT-1	GDGT-2	GDGT-3	Cren'	Cren	GDGT-0				TEX₈₆
DSDP 398-2304	Cretaceous marine sed.[6]	GC	2.6	9.7	2.6	11.6	70.5	2.9				0.9
		LC	6.7	10.7	4.5	14.8	56.5	6.8				0.89
Marine sediment	DSDP 179, 341, mid-Waipara K/Pg[2]	GC	7.1	1.5	0.5	4.1	49.6	37.2				0.46
		LC	2.43	2.12	0.49	0.42	58.86	35.68				0.55

Dnieper cold seep, where the TLE could be analysed directly, were fractionated over alumina using *n*-hexane (apolar fraction), *n*-hexane/DCM (9:1, v:v, ketone fraction) and DCM/MeOH (1:1, v:v, polar fraction). Some of the samples had been subjected to different elution steps prior to elution of the polar fraction (Aquilina et al., 2010). The polar fractions were subsequently purified over silica with hexane/ethyl acetate (1:2, v:v), dried under a gentle flow of N_2, and one aliquot was derivatised to their trimethylsilyl (TMS) derivatives by heating (70 °C, 1 h) with a mixture of N,O-bis(trimethylsilyl)trifluoroacetamide/trimethylchlorosilane (BSTFA/TMCS; 99:1, w/w; 50 μL) and pyridine (50 μL). The reactants were evaporated to dryness under a gentle stream of N_2 (40 °C) and dissolved in 50 μL of cyclohexane for analysis by HTGC-FID (1.0 μL injection) and further diluted as required for HTGC–MS (0.5 μL injection volume). Another aliquot was dissolved in 50–500 μL volumes of *n*-hexane/propan-2-ol (99:1, v:v, HPLC grade, Rathburn Chemicals, Walkerburn, UK), filtered over a 0.45 μm PTFE filter (Thermo Fisher Scientific, Rockwood, TN, USA) and analysed by HPLC–APCI-MS using conditions as described by Hopmans et al. (2016).

2.4. Quantification

The GDGT-0 and crenarchaeol standard (Pearson et al., 2016) was used in varying concentrations from 0.56 to 140 μg/mL. A mixture of three triacylglycerols (TAGs) was used as an internal standard comprising trimyristin (C_{42}), tripalmitin (C_{48}) and tristearin (C_{54}), which were added to samples or to the purified GDGT-0 and crenarchaeol standard, prior to derivatisation with BSTFA/TMCS.

2.5. HTGC-FID

An HP-5890 Series II GC equipped with a cool-on-column inlet (manual injection) and flame ionisation detector was fitted with a VF5-ht capillary column (7 m or 15 m × 0.25 mm × 0.1 μm; Agilent Technologies UK Ltd., UK). The 15 m column was used when better separation of the lower molecular weight compounds was desired, and the 7 m column was used for quantification of iGDGTs and measurement of the ratios of iGDGTs and brGDGTs. Analysis on the 15 m column employed a temperature ramp from 58 °C (1 min hold) to 400 °C at 10 °C/min (10 min hold) and a flow of helium with a constant pressure of 20 psi. With the 7 m column, the starting and final temperatures were the same but a 15 °C/min temperature program and a constant pressure of 15 psi was employed in order to achieve a carrier gas flow that is sufficient for quantitative elution of GDGTs. A final temperature of 400 °C was used to elute iGDGTs on the flat isothermal baseline.

iGDGTs were baseline separated on a short column but brGDGTs co-eluted in one peak. Thus, in order to achieve chromatographic separation of the closely eluting isomers of brGDGTs, an HP 5890 Series IIa gas chromatograph with equilibrated pressure control (EPC) was fitted with a 30 m column and a 1 m × 0.25 mm HT-deactivated silica tubing guard column (Zebron Z-Guard, Phenomenex, UK). Analysis on the 30 m column employed a constant flow of 2 mL/min He, and a temperature ramp from 70 °C (1 min hold) to 400 °C at 3 °C/min (10 min hold). The longer column with a constant carrier gas flow resulted in baseline resolution of the brGDGTs with 0, 1 and 2 rings and allowed integration of the different isomers within these peaks.

The FID used H_2 and air at pressures of 12 and 20 psi on the HP 5890 Series II and Series IIa, respectively, and was operated at 400 °C which was crucial for avoiding condensation of the compounds with high molecular weights on cold spots before reaching the flame for combustion.

A mixture of 10 *n*-alkanes ranging from C_{14} to C_{60} (all Sigma Aldrich, Gillingham, UK) with similar concentrations and eluting at temperatures up to 340 (on the 7 m column) and 400 °C (15 m and 30 m columns), was injected at regular intervals to monitor the chromatography (peak shapes) and quantitative elution (typical responses for the 7, 15 and 30 m columns are shown in Supplementary Fig. S1).

2.6. HTGC–TOF-MS

Analysis was carried out using conditions described by Sutton and Rowland (2012). In brief, an Agilent 6890 gas chromatograph fitted with cool-on-column inlet (track oven, +3 °C) and a VF5-ht Ultimetal capillary column (15 m × 0.25 mm × 0.1 μm; Agilent Technologies UK Ltd., UK) was interfaced via a custom transfer line to a BenchTOF-dx™ reflectron time-of-flight mass spectrometer (Almsco International, Llantrisant, UK). The chromatographic column was connected via a Siltite mini-union to the mass spectrometer using HT-deactivated tubing (nominally 2 m; Zebron Z-Guard, Phenomenex, Macclesfield, UK). Samples (0.5 μL) were manually injected, and the column oven was programmed from 40 to 430 °C at 20 °C/min, with helium used as the carrier gas (constant flow mode, 2.5 mL/min). The transfer line was maintained at 430 °C and the ion source (EI mode, 70 eV) temperature at 380 °C. Data were recorded over the range *m/z* 50–1800.

2.7. Data analysis

HTGC-FID chromatograms were recorded using Clarity software (DataApex, Czech Republic) and HTGC–MS chromatograms were recorded using ProtoTOF™ (Version 1.1.1 Build 7). Integrated areas were obtained from the HTGC-FID chromatograms via Clarity and the open source program CHROMuLAN (PiKRON Ltd., Czech Republic). Data analysis of the peak areas was conducted using R and a built-in linear regression model *lm*. Residuals were plotted using *ggplot2*::*fortify* function as the difference between the measured and the fitted values ($y - \hat{y}$), to investigate whether deviations in values from a 1:1 relationship showed dependencies on their magnitude. The critical level (1.67 σ, L_C) and limit of detection (3.3 σ, L_D), based purely on the standard deviation σ of a blank on the GC (0.08, 0.16 mV, respectively) and the correlation of peak height with injected amounts of GDGT-0 (Supplementary Table 1), result in a theoretical L_C and L_D of 2.77 and 2.81 ng injected on-column. As quantification, however, was based on comparison to an internal standard, L_C and L_D were rather determined as 1.67 and 3.3 σ of the concentration of a typical sample (Bernal, 2014), which is a conservative approach. BIT, TEX_{86} and MBT-CBT values were determined according to the following equations:

$$BIT = \frac{brGDGT - Ia + IIa + IIIa}{brGDGT - Ia + IIa + IIIa + Crenarchaeol} \quad (1)$$

(Hopmans et al., 2004),

$$TEX_{86} = \frac{GDGT - 2 + GDGT - 3 + Cren'}{GDGT - 1 + GDGT - 2 + GDGT - 3 + Cren'} \quad (2)$$

(Schouten et al., 2002),

$$MBT = \frac{brGDGT - Ia + Ib + Ic}{brGDGT - Ia + Ib + Ic + IIa + IIb + IIc + IIIa + IIIb + IIIc} \quad (3)$$

(Weijers et al., 2007),

$$CBT = -Log\left(\frac{brGDGT - Ib + IIb}{brGDGT - Ia + IIa}\right) \quad (4)$$

(Weijers et al., 2007).

(Numbers and letters refer to compound structures in Fig. 1. In all cases, the brGDGTs refer to isomers with methyl groups at the 5- or the 6-position; De Jonge et al., 2014).

3. Results and discussion

3.1. Identification and analysis of iGDGTs, pure standards and environmental samples

The purified standards GDGT-0 and crenarchaeol (Pearson et al., 2016) eluted near or at the maximum temperature (400–430 °C) when examined by HTGC-FID (Fig. 2A) and HTGC–TOFMS (Supplementary Fig. S2). GDGT-0 eluted first; its mass spectrum (Supplementary Fig. S2B), although weaker, was similar in key aspects to that obtained from a lipid extract of *T. waiotapuensis* (Sutton and Rowland, 2012). It showed peaks at m/z 1442 (monoisotopic mass of bis-TMS-derivatised GDGT-0: 1445 Da), most likely derived from the molecular ion of the *bis*-trimethylsilylated compound after loss of hydrogens. It also showed peaks corresponding to $[M^{+\cdot} - 2 \times (CH_3)_3]$ at m/z 1354, possibly $[M^{+\cdot} - CHOSiCH_2(CH_3)_2]$ at m/z 1341 (with some H-transfers) and $[M^{+\cdot} - 2 \times Si(CH_3)_3 + 2H]$ at m/z 1301. Further, fragmentation of the molecule by lateral cleavage into two symmetrical fragments of m/z 722 was observed, although in lower abundance than observed by Sutton and Rowland (2012), who analysed a thermophilic archaeon. The lower abundance of fragments derived from lateral cleavage in the marine GDGT-0 might be related to the parallel arrangement of the biphytanyl chains on the glycerol as opposed to an antiparallel arrangement, in line with recent suggestions (Liu et al., 2018). Asymmetrical cleavage would have resulted in m/z 825 and 619, ions which are present but not prominent. Ions at m/z 129/130/131 were observed, corresponding to the glycerol carbon backbone and a –OTMS group $[CH_2CH_2CH_2OTMS^+]$.

The mass spectrum of the later-eluting crenarchaeol (Supplementary Fig. S2C) was also weak but contained a molecular ion at ca. m/z 1435 and a peak at m/z 1291, consistent with $[M^{+\cdot} - 2 \times Si(CH_3)_3 + 2H]$ for crenarchaeol. This GDGT contains the same number of carbon atoms as GDGT-0, but possesses five rings and thus ten fewer hydrogen atoms. Crenarchaeol is asymmetrical (one biphytanyl chain containing two cyclopentyl and one containing two cyclopentyl and one cyclohexyl moiety). Cleavage akin to the symmetrical cleavage observed in GDGT-0 would thus result in fragments with an m/z of 716 and 718; however, these are not obvious in the spectrum obtained. TMS-derivatised GDGTs can be seen clearly by an extracted ion current of the abundant ion at m/z 129 (Supplementary Fig. S2A). Further, m/z 217 is observed in these spectra and those of GDGTs from the environmental samples, as well as by Sutton and Rowland (2012) and could derive from transfer of a TMS group to one of the carbons of the glycerol backbone resulting in $CH_2CHC(OSi(CH_3)_3)_2^+$ as is observed with hydroxy fatty acids (Rontani and Aubert, 2004).

In the sediment from the cold seep, the fragments m/z 1301, 1299, 1297 and 1296 corresponding to $[M^{+\cdot} - 2 \times Si(CH_3)_3 + 2H]$ confirmed the presence of GDGT-0 and, most likely, GDGT-1, GDGT-2 and GDGT-3 (FID trace Fig. 2B, spectra in Supplementary Fig. S3A, C–E), respectively. This was in agreement with HPLC–APCI-MS measurements of the same sample (Supplementary Fig. S4A). These compounds elute later than GDGT-0, but earlier than crenarchaeol, consistent with the increasing cyclisation and thus inferred decreasing vapour pressures (Gliozzi et al., 1983). GDGT-1, -2 and -3 showed the same fragmentation patterns as GDGT-0, corresponding to the losses of TMS and hydrogen rearrangement, as well as the glycerol fragments at m/z 129/130. Both GDGT-1 and GDGT-2 showed fragments at m/z 720 (monocyclic biphytane), also including m/z 722 (for GDGT-1/-2, one acyclic

biphytane) at low abundance. Other compounds identified included mono- and diether lipids, archaeol and *sn*2-hydroxyarchaeol (Fig. 2B).

In the marine sediment mix, compounds with retention behaviour and mass spectra identical to those of GDGT-0 and crenarchaeol were observed as the largest iGDGT peaks (Fig. 2C, Supplementary S3A,B), and these identities were confirmed by co-injection with purified GDGT-0 and crenarchaeol. A peak eluting after crenarchaeol in the GC-FID chromatogram was tentatively identified as crenarchaeol isomer (Fig. 1). This was further supported by the very high intensities of this peak in a sediment that was known to contain a large amount of this compound (Naafs et al., 2016), and this peak was thus tentatively assigned as crenarchaeol isomer. This identification could not be confirmed by MS due to its very low volatility. GDGT-1, -2, and -3 were also present in the marine sediment mix, as evident from the HPLC–APCI-MS chromatogram (Supplementary Fig. S4B). In the HTGC-FID and HTGC–TOFMS chromatograms, these peaks could be identified based on co-elution with the GDGTs present in the seep sample, and based on their mass spectra, although spectra were weak due to the low abundance of the compounds. Crucially, these identifications and distributions were consistent with the HPLC–APCI-MS data (Supplementary Fig. S4A). A number of other small peaks in this region were observed. These could be due to H-GDGTs or different regio-, stereo-, or other isomers of the GDGTs (Schouten et al., 2013b; Liu et al., 2016). Lower molecular weight compounds identified were fatty acids, *n*-alkanols, sterols, diether lipids, and alkenones (Fig. 2C). Further analyses of more concentrated GDGT fractions by HTGC–MS are thus of particular interest, as the separation that is complementary to that achieved by HPLC could provide crucial information for identification of GDGT-isomers.

3.2. Identification and analysis of brGDGTs in peat

In the peat extract, a small amount of GDGT-0 was observed by HTGC-FID (Fig. 3). A much larger peak eluting at 380 °C was found to represent acyclic brGDGTs (Fig. 1B), which co-eluted in one peak (Fig. 3C). While the major iGDGTs possess increasing numbers of rings (Fig. 1A), which are expected to have a large effect on volatility and thus retention (Gliozzi et al., 1983), the major acyclic brGDGTs differ in only one or two additional methyl branches (14 to 28 mass units, 1–2% of the total molecular mass), such that the observed incomplete resolution was expected. Identification was based on mass spectral fragmentation patterns of brGDGTs, which were similar to those of the iGDGTs: The mass spectra showed evident ions of most likely TMS-derivatised brGDGTs (m/z 1194, 1180 and 1166 for brGDGT-IIIa, -IIa, and -Ia, respectively, Supplementary Fig. S6), as well as ions with the corresponding losses of two $Si(CH_3)_3$ groups and a transfer of two or three hydrogens (m/z 1050, 1036, 1022, Supplementary Fig. S6) and those corresponding to the TMSO group and the three carbons of the glycerol moiety (m/z 129/130/131, Supplementary Fig. S6). Retention times of the acyclic brGDGTs were reversed compared to HPLC retention times and increased with increasing molecular weight. Cyclic brGDGTs (Fig. 1B) were found to elute after the non-cyclic GDGTs (Fig. 1B) and a spectrum of the most abundant cyclic brGDGT was obtained (brGDGT-Ib, m/z 1164/1163, fragmenting to m/z 1019/1020, Supplementary Fig. S6). Other cyclic brGDGTs were present in low abundances but could be seen in the extracted ion current of m/z 129 (Fig. 3C).

HPLC–APCI-MS revealed that the peat possessed a distribution of brGDGTs dominated by brGDGT-Ia, IIa and IIIa (Fig. 1B), with minor amounts of the cyclic brGDGTs Ib and Ic, IIb and IIIb (Supplementary Fig. S5). Analysis on a 30 m column with a 2 m precolumn enabled the partial resolution of these three major brGDGT isomers with zero, one, and two cyclic moieties (Fig. 3B); relative distribu-
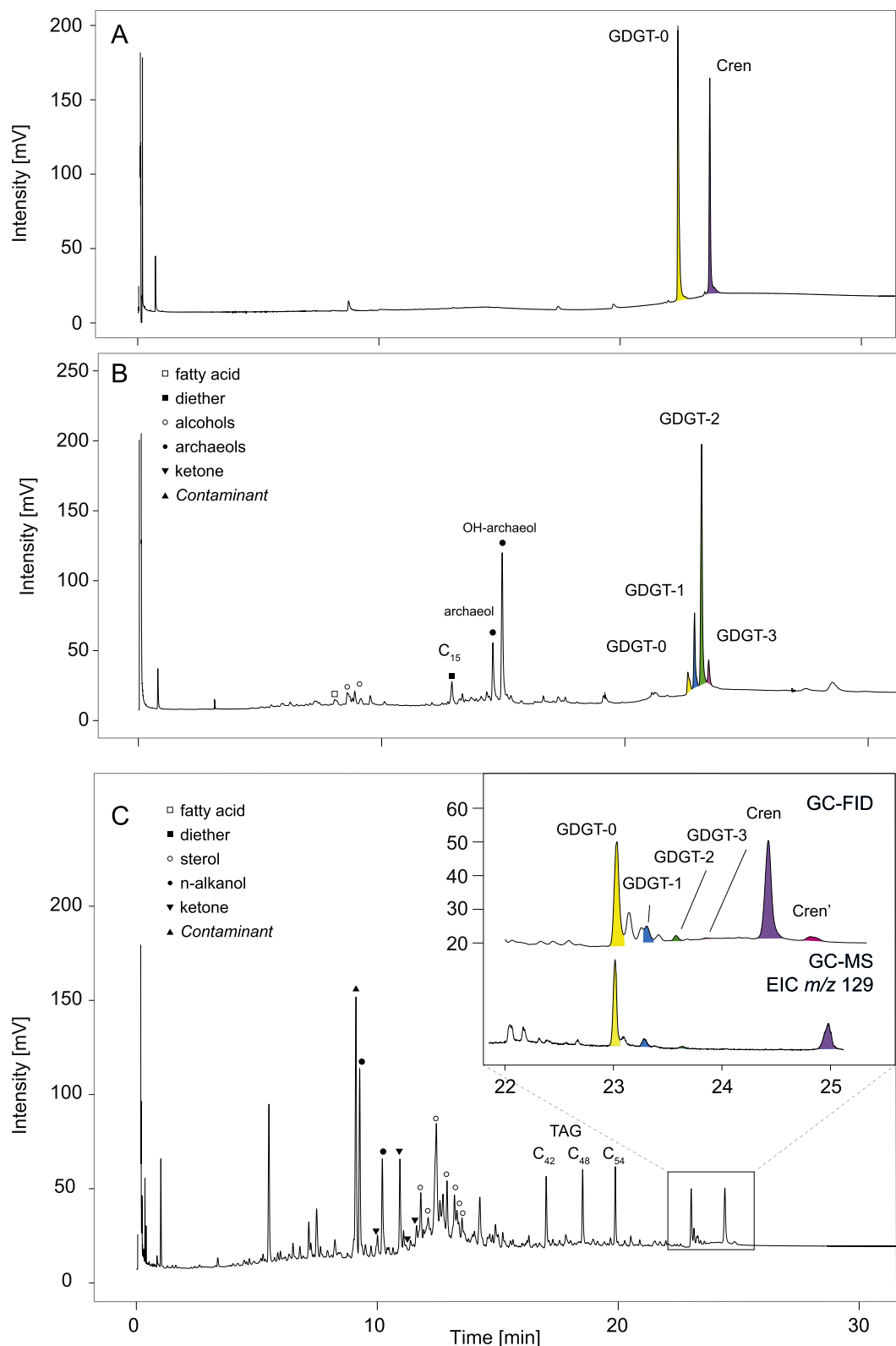
Fig. 2. Partial HTGC chromatograms, showing elution of iGDGTs (and other compounds): A) a 1:1 mixture of GDGT-0 and crenarchaeol purified by preparative HPLC as analysed on a 7 m column, B) sample from a methane seep; C) marine sediment mix, including triacylglycerols added as standards, with enlarged iGDGT-region (insert) and, for comparison, the EIC *m/z* 129 obtained via HTGC-TOFMS. Other compounds detected are indicated. Retention times vary slightly due to shortening of the GC-column as a routine maintenance and lower flow rates necessary for HTGC-TOFMS.

tions were similar to those observed by HPLC–APCI-MS. Optimised chromatography, in particular a slow temperature ramp (3 °C), in addition to a retention gap of 2 m deactivated HTGC tubing,

allowed the partial resolution of three peaks within the first two peak clusters, which were tentatively identified as acyclic isomers with different methylation patterns (Ia, IIa, IIIa; Fig. 1B). The
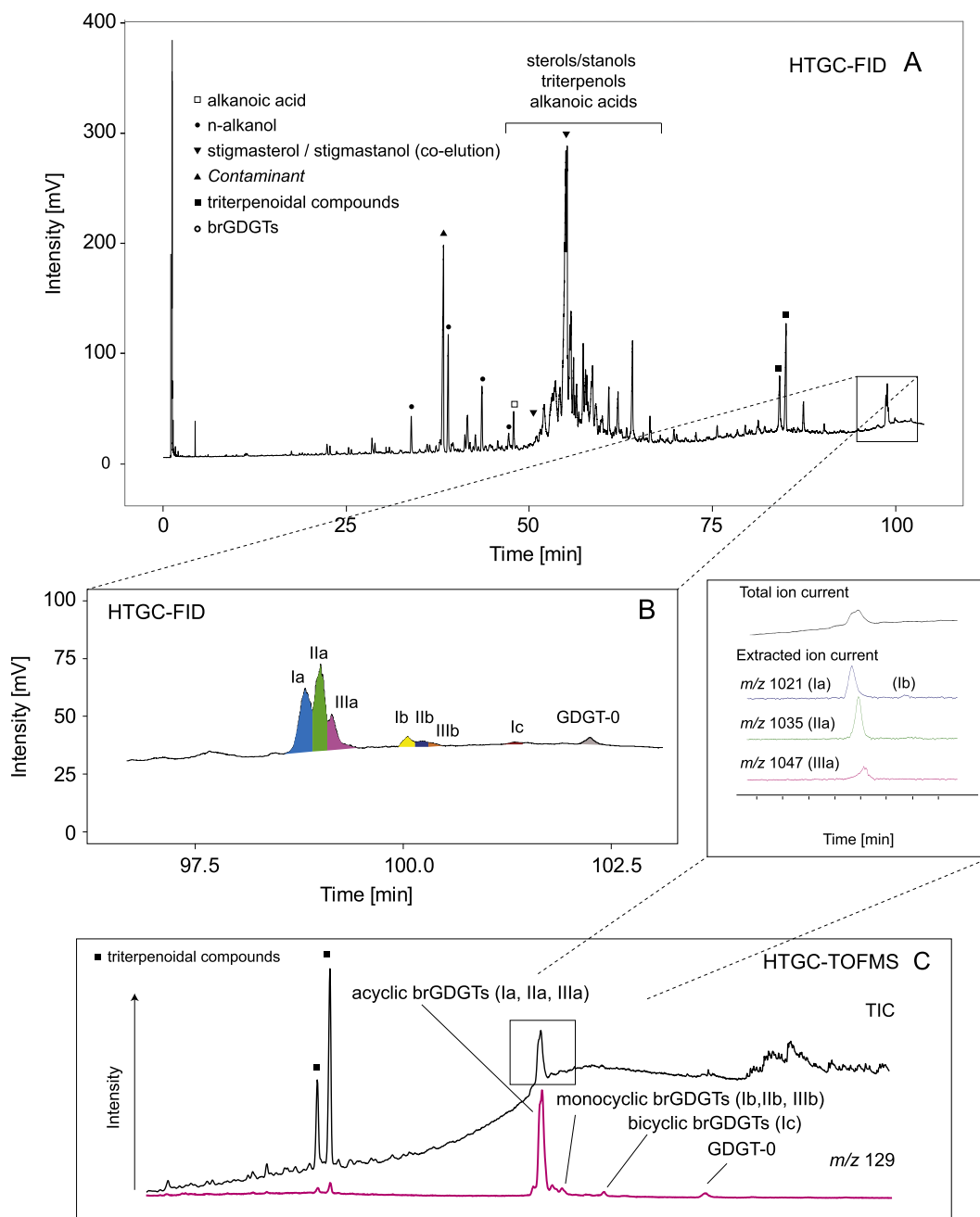
Fig. 3. Partial HTGC chromatograms, showing elution of brGDGTs (and other compounds): A) Peat sample as analysed on a 30 m column; sterols and triterpenoids are also indicated; B) an enlarged region showing elution and separation of different brGDGTs; C) TIC and extracted ion current for m/z 129, showing the brGDGTs and GDGT-0 in the peat sample analysed by HTGC-TOFMS using a 15 m column.

abundances determined by HTGC methods agreed well with the results from HPLC–APCI-MS, as apparent from the single ion chromatograms and the reconstructed TIC of the $[M+H]^+$ of the brGDGTs (Supplementary Fig. S5). However, the HTGC method was not capable of separating the 5- and 6-methylated isomers of the brGDGTs.

Compounds detected in the lower molecular weight range included stigmastanol and stigmasterol, as well as various other triterpenoids and a series of fatty acids. Two unidentified compounds, most probably higher plant triterpenoids, eluted in the higher mass region and were also seen in the extracted ion current of m/z 129 (Fig. 3C). While this most likely represents the mass fragment of the glycerol TMS-ether produced under EIMS conditions, $(CH_3)_3SiOCHCH_2CH^+$, it is also a common fragment produced

by A-ring cleavage in sterols and terpenols (Brooks et al., 1968; Goad and Akihisa, 1997).

3.3. Quantification of GDGTs by GC-FID

Due to lack of sufficient quantities of tetraether standards, the internal standards tested for quantitative estimation of GDGTs were three triacylglycerols (TAG): trimyristin (C_{42}), tripalmitin (C_{48}) and tristearin (C_{54}). The robustness of TAGs quantification via HTGC has been demonstrated previously (Buchgraber et al., 2004). The compounds required warming to ~40 °C in order to ensure quantitative dissolution of the C_{54} TAG. TAGs appear suitable for quantification of GDGTs, as they elute only slightly earlier than brGDGTs, but later than the majority of other biomarkers,

resulting in less likelihood of co-elution with other compounds. This became particularly important when a 7 m column with decreased resolving power was used. Even though all three TAGs are in principle suitable as internal standards, in this case, trimyristin (C_{42}) was used for all calculations, due to the lack of solubility issues and co-eluting compounds in all analysed samples.

GDGT quantification was explored using a solution with a known concentration of GDGT-0 purified from marine sediments (Pearson et al., 2016). Since only small amounts of this standard were available, we conducted only a limited number of quantification experiments. Mixtures of known concentrations of the GDGT-0 standard and TAGs (C_{42}, C_{48} and C_{54}, dissolved to achieve 0.56–140 μg/mL of GDGT-0 and 10–100 μg/mL TAG) were injected. These yielded a linear response across two orders of magnitude of variation in GDGT-0 concentration (area ratio vs injected amount), with a slope of 1.067, an intercept of –0.003 ng and an

R^2 value of 0.99 (Fig. 4A, Supplementary Table 1). The typical relative standard deviation of the peak area ratios was tested with one sample (5.6 μg/mL) and determined to be 1%. This confirms that, even though the GC reaches temperatures of 400 °C, the areas achieved by HTGC-FID for GDGT-0 are directly proportional to its concentration in the same way as triacylglycerols (TAGs).

However, crenarchaeol elutes with a longer retention time than GDGT-0. Three mixtures of GDGT-0 and crenarchaeol were injected to test the effect of high temperatures and possible band broadening effects in the isothermal region on the quantification of the late eluting crenarchaeol. The GDGT-0/Crenarchaeol ratios of these mixtures, ranging from 0.31 to 2.3, were reasonably well reproduced by the HTGC-FID analyses (Fig. 4B), but crenarchaeol abundances were underestimated by on average 14%, implying that some caution is necessary in the isothermal region. This underestimation was more important at low crenarchaeol concentrations
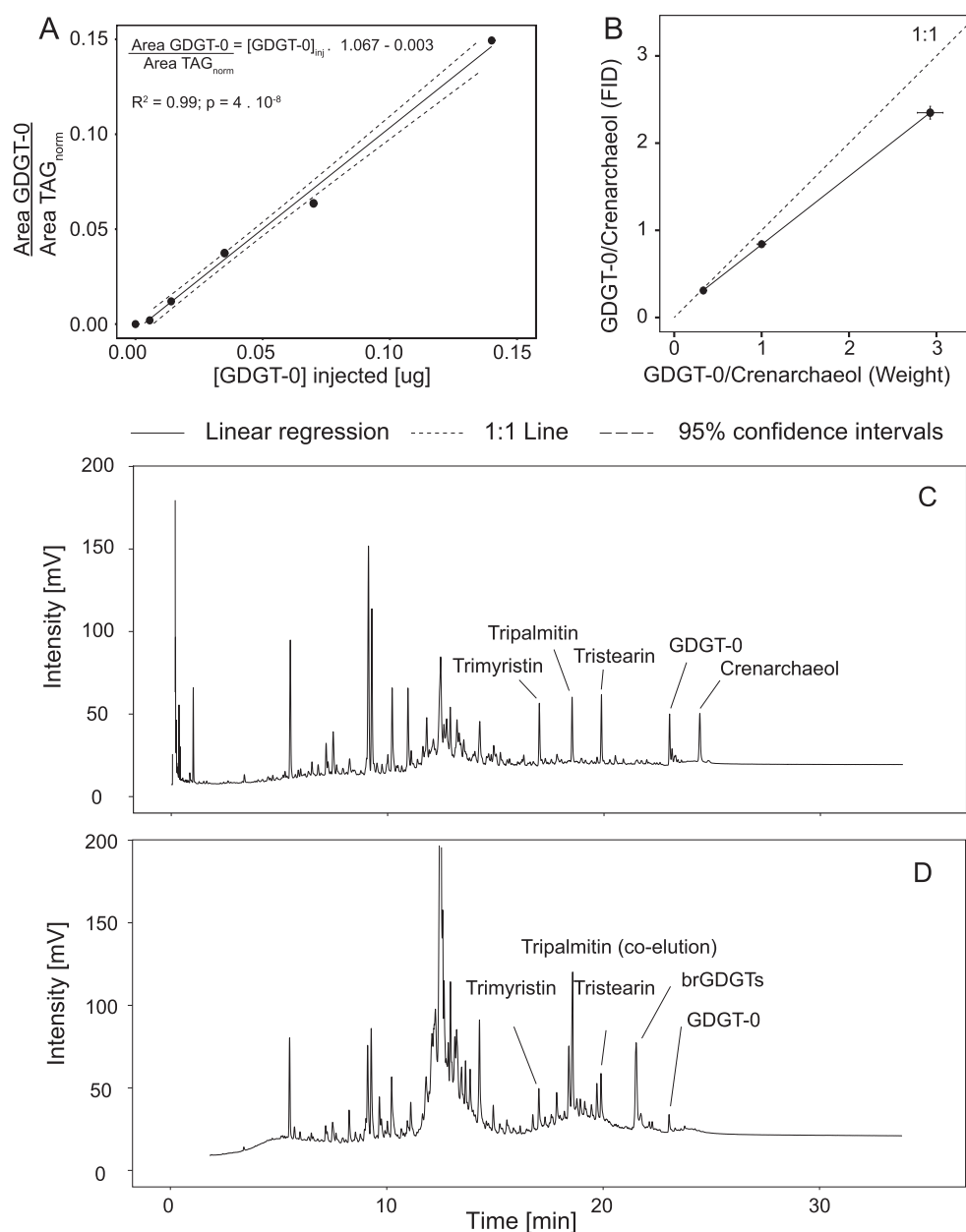

Fig. 4. Quantification of GDGT-0. A) Correlation of Peak area ratios GDGT-0/trimyristin (normalised on μg trimyristin injected) with the amount of GDGT-0 injected in μg; B) Crenarchaeol/GDGT-0 peak area ratios determined from three mixtures of purified compounds of different relative composition (GDGT-0/Crenarchaeol = 1:1, 1:3.1, and 4:1.2); C and D show chromatograms of the peat and marine standards with added TAG standards.

(one-tailed t-test statistically significant at the 95% confidence level, df = 4, for the 2.3 GDGT-0/Crenarchaeol ratio).

Addition of a TAG standard to the marine and peat mixes (Fig. 4CD) allowed the determination of GDGT-0 and crenarchaeol concentrations in samples with 16 (GDGT-0, marine), and 21 ng (crenarchaeol, marine) injected on column, with standard deviations of 1.3 ng (GDGT-0) and 1.4 ng (crenarchaeol) (n = 3). This implies a critical level (L_C) of 2 ng and a limit of detection (L_D) of 4 ng injected on-column (Bernal, 2014) in real samples, which corresponds to an L_D of as low as 20 ng GDGT extracted (extraction techniques were not evaluated here, but have been discussed elsewhere; e.g., Lengger et al., 2012; Chaves Torres and Pancost, 2016). These values are higher than for HPLC–APCI-MS (ca. 0.25 ng on column L_D; Huguet et al., 2006), which employs single ion monitoring with increased sensitivity. The FID-response is linear across the whole temperature range, i.e. between TAGs and GDGT-0 and even between GDGT-0 and crenarchaeol. This suggests that brGDGTs, with retention times approximately equal to those of the triacylglycerols, should also show similarly stable response factors. Consequently, using the same method, mean brGDGT concentrations were determined in the peat extract and were 60 (±5) μg/mL for the acyclic and 10 (±4) μg/mL for the cyclic brGDGTs (n = 4). A disadvantage of the HTGC-FID quantification method, in addition to lower sensitivity, is the potential co-elution of other compounds of high molecular weight. However, HTGC-FID is less dependent on the potentially variable relative response factors between standards and GDGTs that are observed when using HPLC–APCI-MS (Huguet et al., 2006). Most crucially, the determination in a single analysis of abundances of GDGTs and lower molecular weight biomarkers could improve the reliability of some proxies, such as the ratio of archaeol to GDGT-0 (ACE) in hypersaline systems (Turich and Freeman, 2011). In addition, quantitative elution from a HTGC column could, in the future, enable the use of GC coupled to stable isotope ratio monitoring for the determination of $\delta^{13}C$ and δ^2H values of GDGTs and other analytes.

3.4. Biomarker ratios as determined by HTGC – potential and limitations

3.4.1. Branched over isoprenoid tetraether index (BIT)

The BIT index describes the relative amounts of brGDGTs compared to crenarchaeol, with the former being more common in terrestrial and the latter more common in marine environments (Hopmans et al., 2004). BIT indices determined from the same samples have been shown to vary between different laboratories, particularly in the intermediate value range (Schouten et al., 2013a). The extraction and HPLC–APCI-MS protocols and equipment used in this study were similar to those used in the round robin experiments (Schouten et al., 2009, 2013a). Here, mixtures of extracts of the peat sample with a BIT of ~1 (only minor amounts of crenarchaeol) and the marine sediment mixture (BIT = 0.1) were analysed using HPLC–APCI-MS and HTGC-FID, to determine whether the two methods yielded comparable BIT indices. The resulting areas were normalised on the molecular weight of brGDGTs and crenarchaeol in order to reflect the fact that, by definition, BIT is a molar index (Schouten et al., 2013a). Molar BIT indices obtained using HTGC-FID (7 m column method) were well correlated with the values obtained by HPLC–APCI-MS, though slightly higher (Fig. 5A, BIT_{GC} = 0.945 × BIT_{LC} − 0.12, R^2 = 0.98, n = 14 with three of those duplicates). A number of sediment extracts from the Baltic Sea (Aquilina et al., 2010) with a large range of BIT values (0.07–0.82, Table 1) were also analysed. They showed a similar correlation between HPLC–APCI-MS and HTGC-FID determined values (Fig. 5B, BIT_{GC} = 0.979 × BIT_{LC} − 0.05, R^2 = 0.93). Residuals for both datasets were unstructured (Fig. 5C). However, in the case of very low crenarchaeol concentrations, HTGC-FID analyses approached the limit of quantification for crenarchaeol and resulted in elevated BIT values (e.g., 1.0 vs 0.82, Table 1).

We thus report reliable BIT determinations, particularly at high and intermediate crenarchaeol concentrations. These results, with an average BIT difference of 0.08 units and a maximum detected difference of 0.18 units, compare favourably to results from inter-laboratory studies using HPLC–MS techniques, which demonstrated a general limit of reproducibility of 0.410 BIT units (Schouten et al., 2009), and 0.15 BIT units (Schouten et al., 2013a). Therefore, the application of the HTGC-FID method for BIT index determination, in addition to HPLC–APCI-MS, could allow screening for BIT indices in laboratories that only have GC-FID systems before external analysis. It could improve reproducibility and should render the application of correction factors (Schouten et al., 2009) based on mixtures of pure compounds less necessary.

3.4.2. Paleotemperature proxies (MBT-CBT and TEX_{86})

In order to investigate the suitability of the HTGC approach for determination of MBT ratios, we analysed five peats and soils from a global dataset using both approaches (Table 1). As discussed above, brGDGTs are not fully resolved via HTGC-FID, but a suitable resolution for independent integration was obtained using a 30 m column (Fig. 3A,B). BrGDGTs were separated into three groups of peaks, based on the number of rings (Fig. 3B). These groups were baseline resolved on a 30 m column, but individual acyclic and cyclic isomers were only partially resolved. Because the C-5 and C-6 methylated isomers could not be separated, we could not compare the more recently established temperature calibrations, e.g. MATmr (De Jonge et al., 2014). MBT indices generally agreed between the two methods (Fig. 5D, MBT_{GC} = 1.14 × MBT_{LC} − 0.13, R^2 = 0.98). However, the degree of cyclisation, CBT (Fig. 5E), deviated more strongly from a 1:1 correlation (CBT_{GC} = 0.707 × CBT_{LC} − 0.012, R^2 = 0.87). This is not surprising, as MBT is governed by the major isomers of brGDGTs and is less affected by the generally less abundant cyclic brGDGTs and therefore by the higher limit of quantification of the HTGC approach. In contrast, CBT is governed by the cyclopentane ring-bearing components which are present in relatively low abundance.

TEX_{86} determinations were also attempted using all samples of marine provenance. Abundances of the compounds used in this proxy were only high enough in a sample from a Cretaceous marine sediment (Naafs et al., 2016) and an in-house generated marine standard from recent marine sediments (Table 1). In these analyses, TEX_{86} values deviated by between 0.01 and 0.07 units from the values determined by LC–MS. This is comparable to the reproducibility determined in inter-laboratory studies (0.050–0.067, Schouten et al., 2009; 0.023–0.53, Schouten et al., 2013a). However, the low abundances of the compounds used to determine the TEX_{86} ratio in some marine sediment extracts will render a robust determination of TEX_{86} values difficult when using HTGC-FID. The high retention time of the isomer of crenarchaeol in conjunction with the slight discrimination against GDGTs eluting at higher temperatures (Fig. 4B) further complicates the use of this technique for TEX_{86} determinations. This approach is thus not of high enough sensitivity for robust TEX_{86} determinations but could be of use as a screening methodology or to determine other ratios such as GDGT-0/(GDGT-0 + crenarchaeol).

In summary, HTGC-FID can be used to detect suitably derivatised GDGTs. It is possible to use HTGC-FID to determine biomarker ratios of the most abundant GDGTs such as those used to calculate BIT (or MBT) indices. When ratios rely on compounds present in minor amounts such as the crenarchaeol regioisomer for TEX_{86} and cyclic brGDGTs for CBT, the use of HTGC-FID is possible in some cases but produces larger errors. Further, HTGC columns differ depending on the purpose of the analysis, with longer columns required for separation of brGDGTs, and shorter columns to allow
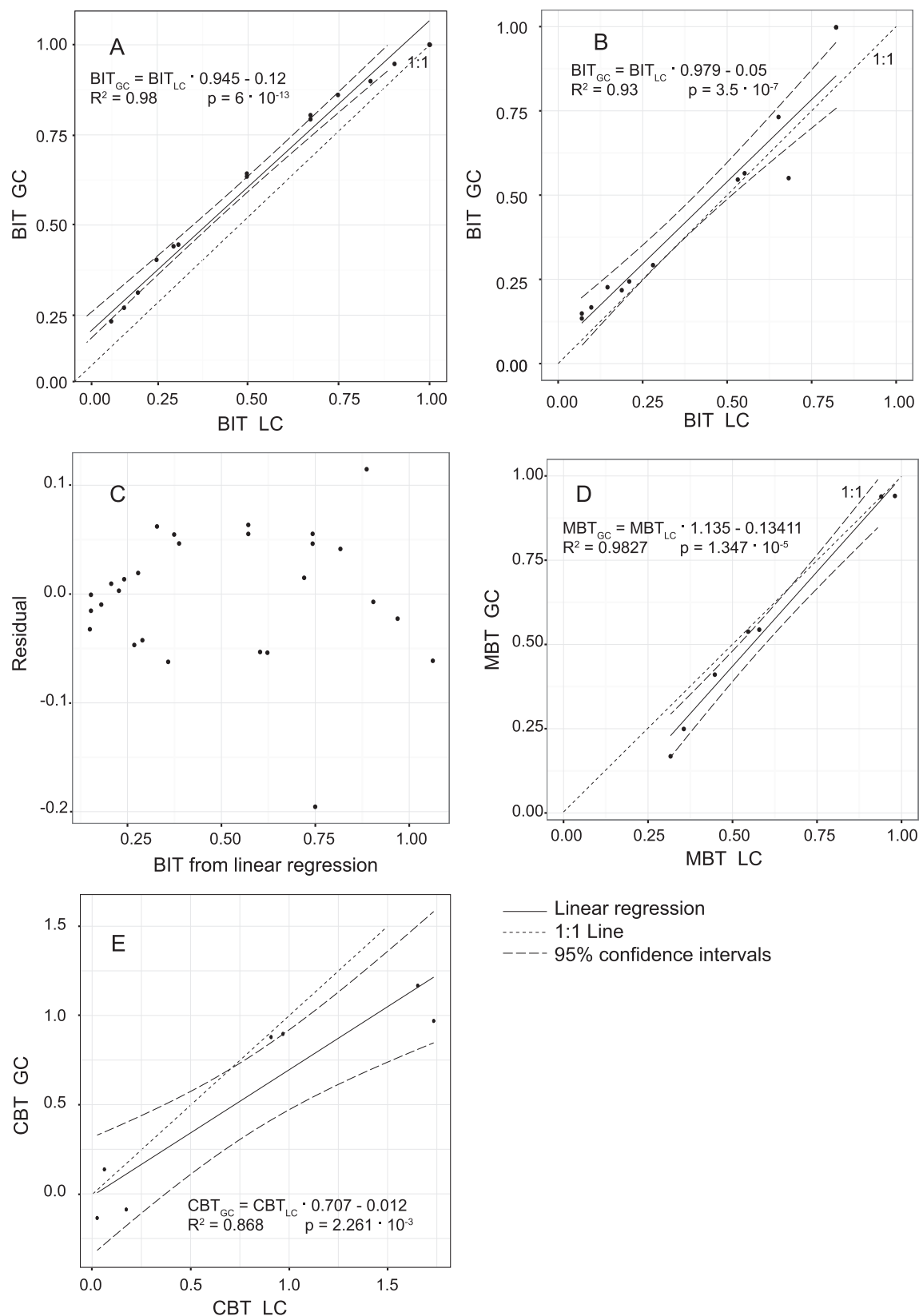
Fig. 5. GDGT-based ratios used in environmental reconstruction, comparing values determined by both HTGC-FID and HPLC-APCI-MS. A) BIT ratios in mixtures of peat and marine standard; B) BIT ratios in samples from the Baltic Sea; C) residual mean error for a linear regression of all BIT samples shown in A and B as plotted versus reconstructed BIT value; D) MBT and E) CBT indices determined from various soil and peat samples. All samples and ratios summarised in Table 1 and Supplementary Table 2. 1:1 ratios, linear regressions and 95% confidence intervals are shown.

elution of iGDGTs. Moreover, HTGC methods are not capable of separating 5- from 6-methylated brGDGTs, of importance in alkaline soils (De Jonge et al., 2014), thus either requiring a pH correction according to Weijers et al. (2007), or restricting use of HTGC to settings where these are known not to occur (e.g., acidic peats; Naafs et al., 2017). Even given those caveats, it is important to note that HTGC-FID lacks the resolving capacity of HPLC–MS approaches and is currently inferior for determining those parameters used in palaeoenvironmental reconstruction. This method, however, could provide new and complementary approaches for identification of GDGTs, families of isomers, and, by extension, of isomers heretofore not identified by LC–MS.

4. Conclusions

The development of HTGC methods, coupled to TOFMS and FID, enabled the identification and quantification of GDGT lipids in environmental samples. Spectra of five iGDGTs and four brGDGTs as TMS-ethers were obtained for the first time by HTGC–TOFMS, employing electron ionisation, and showed consistent fragmentation patterns. Quantification of GDGTs based on an internal standard was fairly robust, with only the latest eluting GDGTs potentially showing discrimination, especially at lower concentrations. Thus, the HTGC-FID approach would alleviate the need for frequent external calibrations with difficult to obtain standards, enable single analysis comparisons of GDGT abundances with those of other compounds usually analysed by GC such as sterols, hopanols, or ether lipids such as archaeol, and present a fairly robust quantification method which could potentially improve inter-laboratory comparability. Currently, HTGC methods are only suitable in a very limited number of cases for the determination of the widely used GDGT-based ratios BIT, MBT-CBT and TEX$_{86}$, but could allow the use of HTGC as a screening method. HTGC methods also can be used as a complementary method in the investigation of GDGT structures and isomers. In addition, the separation and quantitative elution of GDGTs by HTGC, should enable the development of GDGT-specific isotope analyses based on continuous flow methodologies (i.e., HTGC–IRMS).

Acknowledgements

Appendix A. Supplementary material

Supplementary data associated with this article can be found, in the online version, at https://doi.org/10.1016/j.orggeochem.2018.03.012.

*Associate Editor—***Bart van Dongen**

References

Aquilina, A., Knab, N.J., Knittel, K., Kaur, G., Geissler, A., Kelly, S.P., Fossing, H., Boot, C.S., Parkes, R.J., Mills, R.A., Boetius, A., Lloyd, J.R., Pancost, R.D., 2010. Biomarker indicators for anaerobic oxidizers of methane in brackish-marine sediments with diffusive methane fluxes. Organic Geochemistry 41, 414–426.

Bernal, E., 2014. Limit of detection and limit of quantification determination in gas chromatography. In: Guo, X. (Ed.), Advances in Gas Chromatography. InTech. http://doi.org/10.5772/57341.

Bligh, E.G., Dyer, W.J., 1959. A rapid method of total lipid extraction and purification. Canadian Journal of Biochemistry and Physiology 37, 911–917.

Brooks, C.J.W., Horning, E.C., Young, J.S., 1968. Characterization of sterols by gas chromatography-mass spectrometry of the trimethylsilyl ethers. Lipids 3, 391–402.

Buchgraber, M., Ulberth, F., Anklam, E., 2004. Cluster analysis for the systematic grouping of genuine cocoa butter and cocoa butter equivalent samples based on triglyceride patterns. Journal of Agricultural and Food Chemistry 52, 3855–3860.

Chaves Torres, L., Pancost, R.D., 2016. Insoluble prokaryotic membrane lipids in a Sphagnum peat: Implications for organic matter preservation. Organic Geochemistry 93, 77–91.

Dang, X., Yang, H., Naafs, B.D.A., Pancost, R.D., Xie, S., 2016. Evidence of moisture control on the methylation of branched glycerol dialkyl glycerol tetraethers in semi-arid and arid soils. Geochimica et Cosmochimica Acta 189, 24–36.

De Jonge, C., Hopmans, E.C., Zell, C.I., Kim, J.-H., Schouten, S., Sinninghe Damsté, J.S., 2014. Occurrence and abundance of 6-methyl branched glycerol dialkyl glycerol tetraethers in soils: implications for palaeoclimate reconstruction. Geochimica et Cosmochimica Acta 141, 97–112.

De Rosa, M., Gambacorta, A., 1988. The lipids of archaebacteria. Progress in Lipid Research 27, 153–175.

Gliozzi, A., Paoli, G., De Rosa, M., Gambacorta, A., 1983. Effect of isoprenoid cyclization on the transition temperature of lipids in thermophilic archaebacteria. Biochimica et Biophysica Acta – Biomembranes 735, 234–242.

Goad, L.J., Akihisa, T., 1997. Analysis of Sterols. Blackie Academic & Professional, London, New York.

Hopmans, E.C., Schouten, S., Pancost, R.D., van der Meer, M.T.J., Sinninghe Damsté, J.S., 2000. Analysis of intact tetraether lipids in archaeal cell material and sediments by high performance liquid chromatography/atmospheric pressure chemical ionization mass spectrometry. Rapid Communications in Mass Spectrometry 14, 585–589.

Hopmans, E.C., Schouten, S., Sinninghe Damsté, J.S., 2016. The effect of improved chromatography on GDGT-based palaeoproxies. Organic Geochemistry 93, 1–6.

Hopmans, E.C., Weijers, J.W., Schefuß, E., Herfort, L., Sinninghe Damsté, J.S., Schouten, S., 2004. A novel proxy for terrestrial organic matter in sediments based on branched and isoprenoid tetraether lipids. Earth and Planetary Science Letters 224, 107–116.

Hornibrook, E.R.C., Bowes, H.L., 2007. Trophic status impacts both the magnitude and stable carbon isotope composition of methane flux from peatlands. Geophysical Research Letters 34. https://doi.org/10.1029/2007GL031231.

Huguet, C., Hopmans, E.C., Febo-Ayala, W., Thompson, D.H., Sinninghe Damsté, J.S., Schouten, S., 2006. An improved method to determine the absolute abundance of glycerol dibiphytanyl glycerol tetraether lipids. Organic Geochemistry 37, 1036–1041.

Inglis, G.N., Collinson, M.E., Riegel, W., Wilde, V., Farnsworth, A., Lunt, D.J., Valdes, P., Robson, B.E., Scott, A.C., Lenz, O.K., Naafs, B.D.A., Pancost, R.D., 2017. Mid-latitude continental temperatures through the early Eocene in western Europe. Earth and Planetary Science Letters 460, 86–96.

Jensen, S., Neesgaard, V., Skjoldbjerg, S., Brandl, M., Ejsing, C., Treusch, A., 2015. The effects of temperature and growth phase on the lipidomes of Sulfolobus islandicus and Sulfolobus tokodaii. Life 5, 1539–1566.

Knappy, C.S., Chong, J.P.J., Keely, B.J., 2009. Rapid discrimination of archaeal tetraether lipid cores by liquid chromatography-tandem mass spectrometry. Journal of the American Society for Mass Spectrometry 20, 51–59.

Lengger, S.K., Hopmans, E.C., Sinninghe Damsté, J.S., Schouten, S., 2012. Comparison of extraction and work up techniques for analysis of core and intact polar tetraether lipids from sedimentary environments. Organic Geochemistry 47, 34–40.

Liu, X.-L., De Santiago Torio, A., Bosak, T., Summons, R.E., 2016. Novel archaeal tetraether lipids with a cyclohexyl ring identified in Fayetteville Green Lake, NY, and other sulfidic lacustrine settings: Identification of novel archaeal tetraethers with a cyclohexyl ring. Rapid Communications in Mass Spectrometry 30, 1197–1205.

Liu, X.-L., Lipp, J.S., Birgel, D., Summons, R.E., Hinrichs, K.-U., 2018. Predominance of parallel glycerol arrangement in archaeal tetraethers from marine sediments: Structural features revealed from degradation products. Organic Geochemistry 115, 12–23.

Naafs, B.D.A., Castro, J.M., De Gea, G.A., Quijano, M.L., Schmidt, D.N., Pancost, R.D., 2016. Gradual and sustained carbon dioxide release during Aptian Oceanic Anoxic Event 1a. Nature Geoscience 9, 135–139.

Naafs, B.D.A., Inglis, G.N., Zheng, Y., Amesbury, M.J., Biester, H., Bindler, R., Blewett, J., Burrows, M.A., del Castillo Torres, D., Chambers, F.M., Cohen, A.D., Evershed, R.P., Feakins, S.J., Gałka, M., Gallego-Sala, A., Gandois, L., Gray, D.M., Hatcher, P. G., Honorio Coronado, E.N., Hughes, P.D.M., Huguet, A., Könönen, M., Laggoun-Défarge, F., Lähteenoja, O., Lamentowicz, M., Marchant, R., McClymont, E., Pontevedra-Pombal, X., Ponton, C., Pourmand, A., Rizzuti, A.M., Rochefort, L., Schellekens, J., De Vleeschouwer, F., Pancost, R.D., 2017. Introducing global peat-specific temperature and pH calibrations based on brGDGT bacterial lipids. Geochimica et Cosmochimica Acta 208, 285–301.

Nichols, P.D., Shaw, P.M., Mancuso, C.A., Franzmann, P.D., 1993. Analysis of archaeal phospholipid-derived di- and tetraether lipids by high temperature capillary gas chromatography. Journal of Microbiological Methods 18, 1–9.

Pancost, R., Hopmans, E., Sinninghe Damsté, J., 2001. Archaeal lipids in Mediterranean cold seeps: molecular proxies for anaerobic methane oxidation. Geochimica et Cosmochimica Acta 65, 1611–1627.

Pancost, R.D., Coleman, J.M., Love, G.D., Chatzi, A., Bouloubassi, I., Snape, C.E., 2008. Kerogen-bound glycerol dialkyl tetraether lipids released by hydropyrolysis of marine sediments: A bias against incorporation of sedimentary organisms? Organic Geochemistry 39, 1359–1371.

Pearson, A., Hurley, S.J., Walter, S.R.S., Kusch, S., Lichtin, S., Zhang, Y.G., 2016. Stable carbon isotope ratios of intact GDGTs indicate heterogeneous sources to marine sediments. Geochimica et Cosmochimica Acta 181, 18–35.

Pearson, A., Ingalls, A.E., 2013. Assessing the use of archaeal lipids as marine environmental proxies. Annual Review of Earth and Planetary Sciences 41, 359–384.

Roberts, Z.E., Meldrum, F.C., Pancost, R.D., 2008. The archaeal lipid composition of partially lithified cold seep mats. Organic Geochemistry 39, 1000–1006.

Rontani, J.-F., Aubert, C., 2004. Trimethylsilyl transfer during electron ionization mass spectral fragmentation of some ω-hydroxycarboxylic and ω-dicarboxylic acid trimethylsilyl derivatives and the effect of chain length. Rapid Communications in Mass Spectrometry 18, 1889–1895.

Schouten, S., Hoefs, M.J.L., Koopmans, M.P., Bosch, H.-J., Sinninghe Damsté, J.S., 1998. Structural characterization, occurrence and fate of archaeal ether-bound acyclic and cyclic biphytanes and corresponding diols in sediments. Organic Geochemistry 29, 1305–1319.

Schouten, S., Hopmans, E.C., Rosell-Melé, A., Pearson, A., Adam, P., Bauersachs, T., Bard, E., Bernasconi, S.M., Bianchi, T.S., Brocks, J.J., Carlson, L.T., Castañeda, I.S., Derenne, S., Selver, A.D., Dutta, K., Eglinton, T., Fosse, C., Galy, V., Grice, K., Hinrichs, K.-U., Huang, Y., Huguet, A., Huguet, C., Hurley, S., Ingalls, A., Jia, G., Keely, B., Knappy, C., Kondo, M., Krishnan, S., Lincoln, S., Lipp, J., Mangelsdorf, K., Martínez-García, A., Ménot, G., Mets, A., Mollenhauer, G., Ohkouchi, N., Ossebaar, J., Pagani, M., Pancost, R.D., Pearson, E.J., Peterse, F., Reichart, G.-J., Schaeffer, P., Schmitt, G., Schwark, L., Shah, S.R., Smith, R.W., Smittenberg, R.H., Summons, R.E., Takano, Y., Talbot, H.M., Taylor, K.W.R., Tarozo, R., Uchida, M., van Dongen, B.E., Van Mooy, B.A.S., Wang, J., Warren, C., Weijers, J.W.H., Werne, J.P., Woltering, M., Xie, S., Yamamoto, M., Yang, H., Zhang, C.L., Zhang, Y., Zhao, M., Sinninghe Damsté, J.S., 2013a. An interlaboratory study of TEX$_{86}$ and BIT analysis of sediments, extracts, and standard mixtures: TEX$_{86}$ and BIT Index Round Robin. Geochemistry, Geophysics, Geosystems 14, 5263–5285.

Schouten, S., Hopmans, E.C., Schefuß, E., Sinninghe Damsté, J.S., 2002. Distributional variations in marine crenarchaeotal membrane lipids: a new tool for reconstructing ancient sea water temperatures? Earth and Planetary Science Letters 204, 265–274.

Schouten, S., Hopmans, E.C., Sinninghe Damsté, J.S., 2013b. The organic geochemistry of glycerol dialkyl glycerol tetraether lipids: a review. Organic Geochemistry 54, 19–61.

Schouten, S., Hopmans, E.C., van der Meer, J., Mets, A., Bard, E., Bianchi, T.S., Diefendorf, A., Escala, M., Freeman, K.H., Furukawa, Y., Huguet, C., Ingalls, A., Ménot-Combes, G., Nederbragt, A.J., Oba, M., Pearson, A., Pearson, E.J., Rosell-Melé, A., Schaeffer, P., Shah, S.R., Shanahan, T.M., Smith, R.W., Smittenberg, R., Talbot, H.M., Uchida, M., Van Mooy, B.A.S., Yamamoto, M., Zhang, Z., Sinninghe Damsté, J.S., 2009. An interlaboratory study of TEX$_{86}$ and BIT analysis using high-performance liquid chromatography-mass spectrometry. Geochemistry Geophysics Geosystems 10.

Schouten, S., Huguet, C., Hopmans, E.C., Kienhuis, M.V.M., Sinninghe Damsté, J.S., 2007. Analytical methodology for TEX$_{86}$ paleothermometry by high-performance liquid chromatography/atmospheric pressure chemical ionization-mass spectrometry. Analytical Chemistry 79, 2940–2944.

Sehgal, S.N., Kates, M., Gibbons, N.E., 1962. Lipids of *Halobacterium cutirubrum*. Canadian Journal of Biochemistry and Physiology 40, 69–81.

Sjövall, P., Thiel, V., Siljeström, S., Heim, C., Hode, T., Lausmaa, J., 2008. Organic geochemical microanalysis by time-of-flight secondary ion mass spectrometry (ToF-SIMS). Geostandards and Geoanalytical Research 32, 267–277.

Sutton, P.A., Rowland, S.J., 2012. High temperature gas chromatography–time-of-flight-mass spectrometry (HTGC–ToF-MS) for high-boiling compounds. Journal of Chromatography A 1243, 69–80.

Taylor, K.W.R., Huber, M., Hollis, C.J., Hernandez-Sanchez, M.T., Pancost, R.D., 2013. Re-evaluating modern and Palaeogene GDGT distributions: implications for SST reconstructions. Global and Planetary Change 108, 158–174.

Taylor, K.W.R., Willumsen, P.S., Hollis, C.J., Pancost, R.D., 2018. South Pacific evidence for the long-term climate impact of the Cretaceous/Paleogene boundary event. Earth-Science Reviews 179, 287–302.

Turich, C., Freeman, K.H., 2011. Archaeal lipids record paleosalinity in hypersaline systems. Organic Geochemistry 42, 1147–1157.

Weijers, J.W.H., Schouten, S., Hopmans, E.C., Geenevasen, J.A.J., David, O.R.P., Coleman, J.M., Pancost, R.D., Sinninghe Damsté, J.S., 2006. Membrane lipids of mesophilic anaerobic bacteria thriving in peats have typical archaeal traits. Environmental Microbiology 8, 648–657.

Weijers, J.W.H., Schouten, S., van den Donker, J.C., Hopmans, E.C., Sinninghe Damsté, J.S., 2007. Environmental controls on bacterial tetraether membrane lipid distribution in soils. Geochimica et Cosmochimica Acta 71, 703–713.

Wörmer, L., Elvert, M., Fuchser, J., Lipp, J.S., Buttigieg, P.L., Zabel, M., Hinrichs, K.-U., 2014. Ultra-high-resolution paleoenvironmental records via direct laser-based analysis of lipid biomarkers in sediment core samples. Proceedings of the National Academy of Sciences 111, 15669–15674.

Zhu, C., Lipp, J.S., Wörmer, L., Becker, K.W., Schröder, J., Hinrichs, K.-U., 2013. Comprehensive glycerol ether lipid fingerprints through a novel reversed phase liquid chromatography–mass spectrometry protocol. Organic Geochemistry 65, 53–62.